Search for GeV Emission from Gamma-Ray Bursts Using Milagro Scaler Data

David A. Williams for the Milagro Collaboration

A. A. Abdo, B. T. Allen, E. Anzenberg, T. Aune, D. Berley, E. Blaufuss, S. Casanova, B. L. Dingus, R. W. Ellsworth, M. M. Gonzalez, J. A. Goodman, E. Hays, C. M. Hoffman, C. P. Lansdell, J. T. Linnemann, J. E. McEnery, A. I. Mincer, P. Nemethy, D. Noyes, J. M. Ryan, F. W. Samuelson, P. M. Saz Parkinson, A. Shoup, G. Sinnis, A. J. Smith, G. W. Sullivan, V. Vasileiou, G. P. Walker, D. A. Williams, X. W. Xu and G. B. Yodh

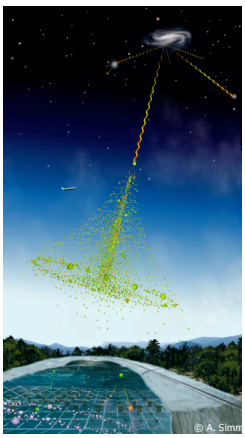

Abstract: Milagro is a wide field (2 sr) high duty cycle (>90%) ground based water Cherenkov detector built to observe extensive air showers produced by high energy particles interacting in the Earth's atmosphere. Milagro records extensive air showers in the energy range 100 GeV to 100 TeV, as well as the counting rates of the individual photomultiplier tubes in the detector. The individual tube counting rates can be used to detect transient emission above ~1 GeV. We have used the counting rate (scaler) data to search for high energy emission from a sample of about one hundred gamma-ray bursts (GRB) detected since the beginning of 2000 by BATSE, BeppoSax, HETE-2, INTEGRAL, Swift or the IPN. No evidence for emission from any of the bursts has been found, and we present fluence upper limits from these bursts.

The Scaler Data Acquisition System:

The single hit rates of all of the PMTs at two different thresholds (a low threshold of ~0.25 photoelectrons and a high threshold of ~4 photoelectrons) are recorded once a second by a CAMAC data acquisition system. To reduce the number of scalers needed to record the rates, tubes are combined into groups of 8 or 16, and the logical "or" of hits from the individual tubes in the group is recorded. In this analysis, we use the low threshold hits in the PMTs in the Milagro top layer. Those PMTs are in groups of 8 such that nearest neighbors are in different groups.

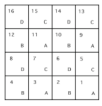

Figure 1 Assignment of PMTs in a 4x4 patch in to the top layer of the pond to or'ed groups of 8. Tubes labeled A and D are in one group; tubes labeled B and C are in another group.

Exclusion of Noisy Channels:

The RMS of the rate for each PMT group is calculated over the 11 day interval around each burst. Noisy channels with an RMS which degrades the signal to noise of the sum are excluded from the analysis for that burst, yielding a "cleaned" rate from the remaining groups.

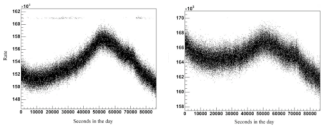

Figure 2 Time history of the rate of a noisy channel (left) and a quiet channel (right). Note the entries at 161,000 in the plot on the left. The trends seen in both plots are from atmospheric pressure and temperature variation.

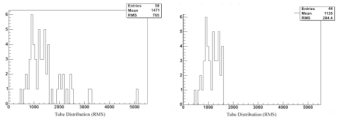

Figure 3 Histogram of the PMT group RMS values for a particular burst before (left) and after (right) removing the noisy groups.

Correction for Pressure and Temperature:

The PMT rates vary as the outside temperature and pressure change the profile of the atmospheric overburden. Linear corrections for temperature and pressure which minimize the overall RMS of the rate (while keeping the average rate unchanged) are calculated for the 11 day interval around each burst.

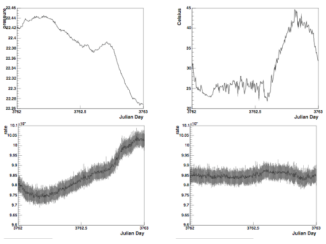

Figure 4 Atmospheric pressure (upper left) and outside temperature (upper right) at Milagro for MJD 53762. The total rate from the top layer PMTs is shown before (lower left) and after (lower right) correcting the rates for the pressure and temperature.

The Milagro Detector:

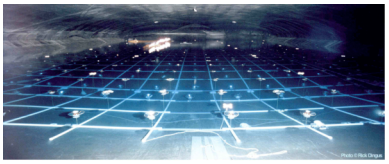

- Located in New Mexico at 2630m above sea level
- 80 m x 60 m light-tight, water-filled pond + outriggers
- 898 photomultiplier tubes (PMTs) detect Cherenkov light from extensive air showers:
  - 450 top layer PMTs used for shower reconstruction (via PMT timing)
  - 273 bottom layer PMTs used for background rejection
  - 175 water tanks (outriggers) improve angular resolution
- 3.4 x 10^4 m² physical area, ~2 sr field of view
- ~1700 Hz trigger rate – due almost entirely to cosmic-ray showers
- ~0.5° angular resolution, > 90% proton rejection
- Near continuous operation since 2000 -- duty factor > 90%

GRB Analysis:

The average PMT rate during the GRB is compared to the average rate during a period immediately before and after the burst (see Figure 5). By doing the same for many comparable test intervals over an 11 day interval around the burst, it seen that fluctuations are neither Poisson nor Gaussian. The excess (or deficit) rate during the GRB interval, relative to the background region, is compared to the distribution of excesses from the test intervals to obtain the significance of the excess — by computing the Gaussian sigma which corresponds to the probability that the excess is a background fluctuation — and the 99% confidence level upper limit on the rate — by computing the amount of signal which must be added to the test intervals so that 99% of them have a larger excess than the GRB interval. The resulting distribution of significances of the excess is shown in Figure 6. The most significant excess is 3.5 standard deviations, with a 2% probability of occurring in a sample of 98; we don't interpret that as evidence for emission and report upper limits for all the bursts.

Figure 5 Schematic time line of the GRB analysis. The GRB duration (rounded up to an integer number of seconds) is represented in red. A background region consisting of 5 times the burst duration before the burst and 5 times the burst duration after the burst is represented in magenta. The 11 day interval (±5 days on either side of the day of the burst) around the burst is partitioned into test intervals of the same duration as the GRB and corresponding background intervals. The ensemble of test intervals is used to interpret the change in scaler rate during the GRB with respect to the background.

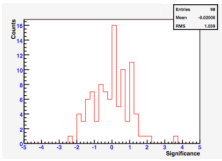

Figure 6 Distribution of significances from the GRB sample. The distribution has a mean very near 0 and an RMS near 1, so the scaler rates during the GRBs in this sample are consistent with fluctuations of the background.

GRB Fluence Limits:

The effective area of the Milagro scalers for gamma rays is calculated using the standard Milagro detector simulation as described in [1], including accounting for any PMTs excluded at the cleaning step. We assume a power law energy spectrum dN/dE ~ E^{-2}, absorbed by collisions with the extragalactic background light according to the model of [2], as shown in Figure 7. For bursts with measured or tentative redshifts, we report limits using EBL absorption for that redshift. For the remaining bursts, we calculate limits for 4 possible redshifts: 0.1, 0.5, 1.0 and 2.0. The *preliminary* fluence limits between 5 and 50 GeV for the unabsorbed power law spectrum are given in Tables 1 and 2. For bursts with redshift >3, we need a more complete model of the EBL absorption below 10 GeV to obtain meaningful limits. The limits are generally comparable to those obtained by this method for other bursts by the ARGO-YBJ [3] group and to the sensitivity expected using this method at Auger [4].

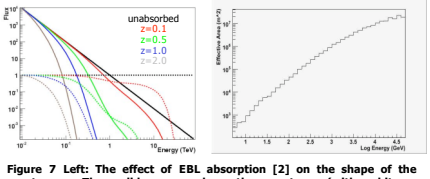

Figure 7 Left: The effect of EBL absorption [2] on the shape of the spectrum. The solid curves show the spectrum (with arbitrary normalization) and the dashed curves show the absorption factor. Right: The effective area of Milagro for detection of a single scaler count as a function of gamma-ray energy for gamma rays incident within 10° of zenith.

TABLE 1. List of GRB in the field of view of Milagro in 2000–2002.

GRB	T90*	θ†	z_{obs}	σ	z=z_{obs}	Upper Limits (5–50 GeV fluence, erg cm^{-2}) z=0.1	z=0.5	z=1.0	z=2.0
000113	370	20.9	–	-1.5	–	3.4e-4	1.3e-3	2.5e-3	6.1e-3
000131	12	40.8	–	-1.4	–	2.6e-5	1.4e-4	3.1e-4	8.5e-4
000205	23	25.2	–	-0.8	–	4.1e-5	1.6e-4	3.3e-4	8.1e-4
000206	10	38.7	–	1.4	–	8.7e-5	4.4e-4	9.4e-4	2.5e-3
000212	8	2.2	–	0.4	–	1.8e-5	6.0e-5	1.2e-4	3.0e-4
000220	3	48.8	–	0.1	–	7.5e-5	4.9e-4	1.0e-3	2.8e-3
000226	10	31.5	–	-0.4	–	2.8e-5	1.2e-4	2.5e-4	6.1e-4
000226b‡	95	32.2	–	0.3	–	8.2e-4	3.6e-3	7.4e-3	1.8e-2
000301c	14	37.6	2.03	0.0	1.7e-3	–	–	–	–
000302	120	31.9	–	-1.3	–	4.1e-4	1.8e-3	3.7e-3	9.0e-3
000314	13	45.3	–	-0.2	–	1.6e-4	9.6e-4	2.1e-3	5.8e-3
000317	550	6.4	–	1.1	–	3.1e-3	1.1e-2	2.1e-2	5.2e-2
000330	1	30.0	–	-0.1	–	4.7e-6	2.0e-5	4.1e-5	9.9e-5
000331	55	38.3	–	0.6	–	9.6e-4	4.8e-3	1.0e-2	2.7e-2
000402	120	47.7	–	0.5	–	4.8e-3	3.0e-2	6.3e-2	1.7e-1
000408	3	31.1	–	-1.4	–	4.4e-6	1.9e-5	3.9e-5	9.4e-5
000424	5	36.2	–	-1.4	–	1.2e-5	5.8e-5	1.2e-4	3.0e-4
000508	30	34.1	–	-2.3	–	1.4e-5	6.2e-5	1.3e-4	3.2e-4
000607‡	1	41.8	–	3.5	–	6.7e-5	3.7e-4	8.3e-4	2.4e-3
000615	10	39.0	–	-1.9	–	1.1e-5	5.7e-5	1.2e-4	3.2e-4
000630	20	33.2	–	0.9	–	1.3e-4	5.8e-4	1.2e-3	2.9e-3
000707‡‡	18	42.5	–	0.6	–	1.7e-4	9.6e-4	2.2e-3	6.3e-3
000727	10	40.8	–	0.2	–	5.3e-5	2.8e-4	6.3e-4	1.7e-3
000730	7	19.2	–	-0.7	–	7.3e-6	2.7e-5	5.4e-5	1.3e-4
000821‡	140	26.5	–	-0.4	–	6.3e-4	2.5e-3	5.2e-3	1.3e-2
000830‡	8	34.6	–	0.3	–	2.5e-5	1.1e-4	2.4e-4	5.9e-4
000926	25	15.9	2.04	-1.2	3.5e-4	–	–	–	–
001017	10	42.1	–	-0.2	–	5.4e-5	3.0e-4	6.8e-4	2.0e-3
001018	31	31.8	–	1.1	–	8.0e-5	3.5e-4	7.2e-4	1.8e-3
001019	10	19.5	–	-1.3	–	6.0e-6	2.2e-5	4.4e-5	1.1e-4
001022	1	37.8	–	0.0	–	9.3e-6	4.6e-5	9.8e-5	2.5e-4
001105	30	8.5	–	1.3	–	4.0e-5	1.4e-4	2.7e-4	6.6e-4
001204	1	47.8	–	-1.9	–	6.6e-6	4.1e-5	8.7e-5	2.3e-4
010104	2	19.8	–	1.1	–	1.1e-5	4.0e-5	8.0e-5	1.9e-4
010220	150	27.0	–	-1.3	–	8.5e-5	3.4e-4	7.0e-4	1.7e-3
010613	152	24.7	–	0.8	–	6.0e-4	2.3e-3	4.8e-3	1.2e-2
010706	48	37.3	–	-0.7	–	2.0e-4	9.8e-4	2.1e-3	5.3e-3
010903	41	48.5	–	1.2	–	1.6e-3	1.0e-2	2.2e-2	5.9e-2
010921	25	10.4	0.45	0.6	4.0e-4	–	–	–	–
011130	84	33.7	–	-0.6	–	3.0e-4	1.4e-3	2.8e-3	6.9e-3
011212	85	33.0	–	0.1	–	2.8e-4	1.2e-3	2.6e-3	6.3e-3
020311	12	27.1	–	0.6	–	3.2e-5	1.3e-4	2.6e-4	6.4e-4
020429‡‡	16	38.5	–	-0.6	–	4.1e-5	2.1e-4	4.5e-4	1.2e-3
020702	26	34.2	–	1.4	–	9.3e-5	4.3e-4	8.9e-4	2.2e-3
020908‡	17	19.2	–	0.0	–	2.8e-5	1.0e-4	2.0e-4	4.8e-4
020914	9	5.7	–	-1.2	–	6.3e-6	2.1e-5	4.2e-5	1.1e-4
021104	20	13.3	–	1.1	–	5.0e-5	1.7e-4	3.3e-4	7.7e-4
021112	8	33.6	–	-0.4	–	2.4e-5	1.1e-4	2.2e-4	5.4e-4
021113	20	17.6	–	-1.2	–	2.1e-5	7.7e-5	1.5e-4	3.7e-4
021211	6	34.8	–	0.3	–	2.0e-5	9.1e-5	1.9e-4	4.7e-4

‡The IPN localized this burst to two disconnected regions, only one of which was in the Milagro field of view

‡‡The IPN localized this burst to two disconnected regions, both in the Milagro field of view; the limit assumes the burst was in the lower elevation region

TABLE 2. List of GRB in the field of view of Milagro in 2003–mid-2006.

GRB	T90*	θ†	z_{obs}	σ	z=z_{obs}	Upper Limits (5–50 GeV fluence, erg cm^{-2}) z=0.1	z=0.5	z=1.0	z=2.0
030413	15	27.1	–	-1.7	–	1.1e-5	4.5e-5	9.2e-5	2.2e-4
030823	56	33.4	–	0.2	–	2.4e-4	1.1e-3	2.2e-3	5.5e-3
031026	1	45.3	–	1.0	–	3.7e-5	2.2e-4	4.8e-4	1.3e-3
031220	24	43.4	–	0.1	–	1.2e-4	7.1e-4	1.6e-3	4.6e-3
040506	175	48.7	–	-1.6	–	2.0e-3	1.3e-2	2.8e-2	7.3e-2
040924	1	43.3	–	-0.5	–	1.5e-5	8.8e-5	2.0e-4	5.7e-4
041211	31	43.0	–	1.5	–	2.0e-4	1.2e-3	2.6e-3	7.5e-3
041219a	520	26.9	–	1.5	–	1.7e-3	7.0e-3	1.4e-2	3.5e-2
050124	4	23.0	–	-0.6	–	6.0e-6	2.3e-5	4.6e-5	1.1e-4
050213	17	22.6	–	-0.4	–	1.4e-5	5.4e-5	1.1e-4	2.6e-4
050319	15	45.1	3.24	1.2	–	–	–	–	–
050402	8	40.4	–	-1.0	–	2.3e-5	1.2e-4	2.7e-4	7.4e-4
050412	26	37.1	–	0.2	–	5.6e-5	2.7e-4	5.8e-4	1.5e-3
050502	20	42.7	3.793	-1.1	–	–	–	–	–
050504	80	27.6	–	0.5	–	2.0e-4	8.0e-4	1.6e-3	4.0e-3
050505	60	28.9	4.3	-2.0	–	–	–	–	–
050509b	1	10.0	0.2267	-0.5	4.3e-6	–	–	–	–
050522	15	22.8	–	-0.1	–	1.8e-5	6.7e-5	1.4e-4	3.3e-4
050607	27	29.3	–	1.0	–	5.1e-5	2.1e-4	4.4e-4	1.1e-3
050703	26	26.0	–	0.1	–	4.7e-5	1.9e-4	3.8e-4	9.3e-4
050712	35	38.8	–	0.6	–	1.7e-4	8.7e-4	1.9e-3	5.0e-3
050713b	30	44.2	–	0.2	–	2.6e-4	1.5e-3	3.3e-3	9.4e-3
050715	52	36.9	–	0.2	–	2.6e-4	1.2e-3	2.6e-3	6.7e-3
050716	69	30.3	–	0.7	–	3.1e-4	1.3e-3	2.7e-3	6.5e-3
050820	20	21.9	2.612	-0.3	8.4e-4	–	–	–	–
051103	1	49.9	0.0017	0.4	2.5e-5	–	–	–	–
051109	36	9.6	2.346	1.2	1.8e-3	–	–	–	–
051111	20	43.7	1.55	0.1	3.1e-3	–	–	–	–
051211b	80	33.3	–	0.2	–	3.9e-4	1.7e-3	3.6e-3	8.8e-3
051221	2	41.8	0.55	0.2	1.6e-4	–	–	–	–
051221b	61	25.9	–	-1.0	–	1.5e-4	6.1e-4	1.2e-3	3.0e-3
060102	20	39.9	–	1.2	–	1.3e-4	6.6e-4	1.5e-3	3.9e-3
060109	10	22.4	–	-0.8	–	9.4e-6	3.6e-5	7.3e-5	1.8e-4
060110	15	43.0	–	-1.0	–	5.2e-5	2.9e-4	6.6e-4	1.9e-3
060111b	59	36.5	–	1.0	–	4.6e-4	2.2e-3	4.6e-3	1.2e-2
060114	100	40.6	–	-1.9	–	2.7e-4	1.5e-3	3.2e-3	8.8e-3
060204b	134	30.5	–	2.2	–	7.8e-4	3.3e-3	6.8e-3	1.7e-2
060210	5	43.4	3.91	-0.6	–	–	–	–	–
060218	2000	43.7	0.03	0.0	1.3e-1	–	–	–	–
060306	30	46.2	–	1.2	–	5.9e-4	3.5e-3	7.6e-3	2.1e-2
060312	30	43.6	–	0.0	–	3.9e-4	2.2e-3	5.0e-3	1.4e-2
060313	1	46.7	–	0.6	–	3.9e-5	2.4e-4	5.0e-4	1.4e-3
060403	25	27.6	–	-0.3	–	3.4e-5	1.4e-4	2.9e-4	7.0e-4
060427b	1	16.4	–	0.7	–	4.4e-6	1.6e-5	3.1e-5	7.4e-5
060428b	58	26.6	–	-0.7	–	1.2e-4	5.0e-4	1.0e-3	2.5e-3
060507	185	47.1	–	0.6	–	9.2e-3	5.6e-2	1.2e-1	3.2e-1
060510b	300	42.5	4.9	-0.8	–	–	–	–	–
060515	52	41.5	–	0.2	–	5.0e-4	2.7e-3	6.0e-3	1.7e-2

* Rounded up to an integral number of seconds

† Zenith angle of burst at Milagro, in degrees

References:

[1] Atkins, R. et al. 2003, Ap. J. **595**, 803; Atkins, R. et al. 2005, Ap. J. **630**, 996.
[2] Primack, J. R. et al. 2005, AIP Conf. Proc. **745**, 23.
[3] Di Sciascio, G. et al. 2006, Proc. Multi-Messenger Approach To High Energy Gamma-Ray Sources, Barcelona 2006; astro-ph/0609317.
[4] Allard, D. et al. 2005, Proc. 29th ICRC (Pune); astro-ph/0508441.

UC SANTA CRUZ